STOCKHOLM UNIVERSITY

DEPARTMENT OF PHYSICS

SIMULATION OF THE SCATTERING IN A THORIUM FOIL OF 0.15 - 2.3 MeV ELECTRONS AND POSITRONS

CHR. BARGHOLTZ, L. HOLMBERG, D. LILJEQUIST
and P.-E. TEGNÉR

USIP Report 93-01 January 1993

SIMULATION OF THE SCATTERING IN A THORIUM FOIL OF 0.15 - 2.3 MeV ELECTRONS AND POSITRONS

Chr.Bargholtz, L.Holmberg, D.Liljequist and P.-E.Tegnér
Department of Physics, Stockholm University
Box 6730, S-113 85 Stockholm, Sweden

Abstract
Studies of the scattering in thorium of electrons emitted in the decay of ^{90}Sr, involving measurements of the coincidence spectra of electrons and positrons in the energy region 210 - 420 keV in search for anomalies, have previously been reported. In the analysis of the experimental results, computer simulations of the scattering and energy loss of the electrons and positrons were used. The present report describes the models and assumptions used in this simulation and the comparison with experimentally determined spectra.

Introduction

A number of recent papers have presented results from the search for anomalies in the spectra of positrons and electrons scattered in thorium and certain other heavy elements. Anomalies in the spectra of positrons were first reported by Erb *et al* [1]. In some of the papers, Refs.[2], [3] and [4], part of the analysis consists of a comparison of experimental and computer-simulated results. This method is motivated by the fact that the coincidence spectra observed are substantially influenced by the multiple scattering and energy loss suffered by the electrons and positrons.

We present here a more detailed discussion of the scattering and energy loss of the electrons and the positrons in the experiment reported in ref.[4], and a brief description of the procedures used in simulating these processes.

Experimental geometry

The experimental geometry described in Ref.[4] is shown schematically in Fig.1. A very thin ^{90}Sr source is placed at a distance 8 mm from a thorium foil with the thickness 12.5 μm. The foil, which has the shape of a rectangle of the approximate size 12 x 20 mm, is mounted in a metal ring with 20 mm diameter, placed at the source position of an electron spectrometer. The electron spectrometer faces the same side of the foil as the ^{90}Sr source, the "B" (backscattering) side. The foil is simultaneously at the source position of a positron spectrometer facing the opposite side of the foil (the "T" - transmission - side), thus making possible the measurement of electron-positron coincidences. Both spectrometers are cylindrical magnetic lenses with the acceptance angle $\theta \approx 30^0 \pm 3^0$ relative to the normal to the respective foil surfaces. The relative momentum resolution is 4.5 %. For the measurement of electron-electron coincidences, the positron spectrometer is converted to an electron spectrometer by means of reversing the current.

The ^{90}Sr source is deposited at the bottom of a cylindrical cavity with the diameter 2 mm and the depth 2 mm (Fig.1). This cavity is drilled in a lead-covered steel cylinder, which we will refer to as the "source holder". The outer diameter of the source holder is 5 mm.

Simulation of source decay processes

The decay scheme is shown in Fig.2. The beta decay from ^{90}Sr to ^{90}Y is here named β_1 and has the endpoint energy 0.546 MeV. The decay β_2 from ^{90}Y to ^{90}Zr has the endpoint energy 2.284 MeV. The decay β_3, with endpoint energy 0.5232 MeV, is in itself negligible (branching ratio 0.011 %); however, the E0 decay of ^{90}Zr is of importance in the present context, since, with a probability of about 31 %, it results in the emission of a coincident electron-positron pair with sum kinetic energy 0.739 MeV. The radiation from the source is

thus, for our purposes, dominated by the electrons from the β_1 and β_2 decays, with, in addition, a small number of coincident electron-positron pairs from the E0 decay.

Expressions for the β_1 and β_2 electron energy distributions were obtained from Ref.[5]. The distributions are shown graphically in Fig.3. In the Monte Carlo simulation, the energy of the emitted electron is sampled from these spectral shapes by means of the rejection method. The initial direction of motion of the electron is assumed to be random.

We next consider the energy and direction distribution of the coincident electron and positron emitted in the E0 decay. Let the two leptons be numbered "1" and "2". Their energies, including rest mass energy, are E_{t1} and E_{t2}, i.e. $E_{t1} + E_{t2} = E_{sum} = 1.761$ MeV. Assume that lepton nr 1 has started in a random direction, denoted by the unit vector $\mathbf{d}_1$, with energy $E_{t1} \pm dE_{t1}/2$. The probability for this to happen and for the lepton nr 2 to simultaneously start in a direction $\mathbf{d}_2$, at an angle $\theta \pm d\theta/2$ relative to $\mathbf{d}_1$, is written as $P_{E0}(E_{t1}, G)dE_{t1}dG$, where $G = \cos\theta$. From Ref.[6] is obtained the expression

$$P_{E0}(E_{t1}, G) = Cy[E_{t1}(E_{sum} - E_{t1}) + Gy - 1]dE_{t1}dG \tag{1a}$$

where E_{sum}, E_{t1} and E_{t2} are in units of the electron rest mass, and

$$y = \sqrt{(E_{t1}^2 - 1)(E_{sum} - E_{t1})^2 - 1} \tag{1b}$$

The variable ranges are

$$-1 \leq G \leq 1 \tag{1c}$$

$$E_{sum} = 1.761/0.511 = 3.446 \tag{1d}$$

$$1 \leq E_{t1} \leq 2.446 \tag{1e}$$

The constant C is here arbitrary (> 0), since the sampling of E_{t1} and G is made with the rejection method. A rejection sampling test is shown graphically in Fig.4. Coulomb distortion effects are negligible in this case, as shown in Ref.[7].

Main characteristics of the multiple elastic scattering and energy loss processes

Electrons and positrons are deflected mainly by means of elastic scattering in the screened Coulomb fields of the nuclei in the penetrated material. The average deflection per unit path length, which is shared between multiple small angle scattering events and more occasional large angle scattering events, is conveniently characterized in terms of the transport mean free path λ_{tr}, which may be regarded as the path length on which the correlation with the original direction of motion is substantially lost. Thus, for a particle beam normally incident on a foil of thickness d one finds, assuming that there is no change in λ_{tr} during penetration, that transmission and backscattering are both ≈ 50 % when $d = 2\lambda_{tr}$ [8].

In practice, the transport mean free path depends on the kinetic energy E of the particle. The transport mean free path for electrons in metallic thorium is ≈ 33.0 μm at the energy 0.7 MeV, ≈ 12.0 μm at 0.35 MeV, and ≈ 5.3 μm at 0.2 MeV. The positron values are similar. Since the energy loss during penetration of the thorium foil typically is rather small (see below), one may roughly visualize the scattering by comparing these values with the thickness 12.5 μm of the thorium foil.

At the present electron energies, energy loss in a solid occurs mainly through so-called electronic collisions, i.e. excitation of collective modes of electronic motion or excitation of single electrons to higher, unoccupied levels in the solid. The average energy transfer in such a collision is of the order of 10 eV. A minor part (less than 10 %) of the energy loss is due to radiative collisions, i.e. bremsstrahlung.

Occasionally, electronic collisions occur where an energy transfer much larger than the binding (or Fermi) energy is made from the incident electron or positron to a single bound (or conduction) electron, which

then becomes a high energy secondary electron. In the usually applied cross section formula for such close, binary collisions - referred to as Møller scattering, when the incident particle is an electron, and Bhabha scattering, when the incident particle is a positron - the target electron is assumed (as an approximation) to be initially free and at rest. The change of direction of motion may be large in Møller and Bhabha scattering; nevertheless, the *total* contribution from inelastic collisions to the inverse transport mean free path is small, compared to the contribution from elastic collisions, and may be neglected here.

A substantial part of the energy loss is due to multiple small-loss events. Therefore, the average energy loss per unit path length, i.e. stopping power, is a quantity useful for approximately characterizing the energy loss process. The stopping power for electrons is $\approx$ 1.5, 1.4 and 1.3 keV/μm at the energies 0.2, 0.35 and 0.7 MeV, respectively. The values for positrons are similar. The energy loss for electrons or positrons traversing the thorium foil should thus be of order 1.4 [keV/μm]·12.5 [μm]·1.5 $\approx$ 0.03 MeV, where the factor 1.5 roughly accounts for path length increase due to scattering.

A survey of scattering processes in source holder and foil

The experimental data are analysed in the form of coincidence matrices, e.g. as electron-positron coincidence matrices $M(S_e, S_p)$. Here, S_e and S_p are spectrometer settings corresponding to electron (e) and positron (p) kinetic energies. A matrix element $M(S_e, S_p)$ is the number of recorded coincidences at the settings (S_e, S_p).

Those electrons or positrons which, emitted by nuclei in the source, eventually hit the thorium foil, will have energy distributions influenced by the following scattering processes:

1) Scattering in the source layer itself, which however is neglected since this layer is very thin.

2) Due to the random initial direction of motion, 50 % of the leptons are initially moving inwards from the source surface, into the bottom of the cavity. A considerable fraction of these leptons are backscattered and will reach the foil (see Fig.1), but their energy distribution is then shifted to lower energies and rather strongly smeared out (i.e. they are convoluted with the rather broad energy loss distributions characteristic for electrons backscattered from bulk matter).

3) The solid angle within which the foil is seen from the source is about 10 % of 2π. Thus, $\sim$ 10 % of the leptons escaping from the source hit the foil directly, while $\sim$ 90 % hit the cylindrical walls of the source holder cavity. (See Fig.1; the precise values are influenced by the fact that the angular distribution of those leptons which are backscattered from the bottom of the cavity is not isotropic.) Part of the electron-positron coincidence matrix is therefore due to pairs where at least one lepton has first been scattered from the cavity walls. However, since only a fraction of these leptons escape from the cavity walls, and then, in general, with a substantial energy loss, it turns out that the magnitude of this contribution is much smaller than the percentages mentioned above would seem to indicate.

Apart from hypothetical events in the foil [4], we should observe electron-positron coincidences due to the following processes.

a) The positron from the E0 decay is transmitted through the thorium foil, while the coincident electron from the same decay is backscattered from the foil (Fig.5a).

b) A secondary electron, obtained through Bhabha scattering of a positron from the E0 decay, is ejected from the foil at the source side, while the positron is transmitted (Fig.5b). However, this process is negligible compared to that in Fig.5a, since Bhabha events involving energy transfers large enough to place the electron within our coincidence matrix are, by comparison, very improbable.

c) Coincidence between the positron from the E0 decay (transmitted through the foil) and the electron from the β_3 decay (backscattered). The probability of observing this event is however negligible since the time window [4] is much smaller than the lifetime of the excited ^{90}Zr state.

It thus follows that only (a) needs to be taken into account. This contribution to the electron-positron coincidence matrix will be a "ridge" corresponding to a sum kinetic energy 0.739 MeV, with a certain shift and smearing towards lower energies due to energy losses in the source holder and the foil, as indicated in Fig.6a.

In addition, we consider the hypothetical events in the foil. Such an event is assumed to consist in an electron and a positron starting with equal energies in opposite directions from the same location in the foil [4]. The contribution to the electron-positron coincidence matrix from such events should be a point (peak) with tails due to energy loss in the foil (Fig.6b). For the comparison with experimental electron-positron coincidence data a weighted combination of the simulated matrices schematically shown in Fig.6a and 6b is used [4].

For the purpose of estimating an upper limit of the cross section for the hypothetical events in the foil, electron-electron coincidences were also measured [4]. For the analysis, the electron-electron coincidence matrix corresponding to the scattering geometry in Fig.5c was simulated. Electron-electron coincidences (at energies $\sim 0.1 - 1$ MeV) are due to the occurrence of Møller scattering during the multiple scattering process (i.e. close electron-electron collisions for which the Møller cross section is an appropriate approximation), hence this matrix is subsequently referred to as the Møller coincidence matrix. The probability for the occurrence of such a close collision during one trajectory turns out to be much less than unity (of order 10^{-2}); thus, the possibility of more than one can be disregarded. The coincidence matrix is influenced by multiple scattering and energy loss of both electrons.

In order to check the accuracy of the simulations, singles spectra (which easily provide superior statistical accuracy) were measured and simulated for electrons transmitted through and backscattered from the foil [4]. The scattering processes are indicated in Fig.5d. One should note that the multiple scattering geometry is the same as in Fig.5a, apart from the rather minor differences between positron and electron multiple scattering. Thus, the comparison of measured and simulated singles spectra is an adequate check of the accuracy of the models used to simulate the coincidence matrices.

Survey of programs

Four main programs were used, here called S, E, M and H.

1) Program S is used to simulate singles energy spectra of electrons transmitted and backscattered in the thorium foil (the process in Fig.5d).

2) Program E is used to simulate data for the electron-positron coincidence matrix obtained from the E0 decay (Figs.5a and 6a).

3) Program M is used to simulate data for the electron-electron coincidence matrix obtained by Møller scattering (Fig.5c).

4) Program H is used to simulate data for the electron-positron coincidence matrix obtained from the hypothetical events in the thorium foil (Fig.6b).

All four programs are based on the Fortran codes RELECN and RELPOSN, which perform Monte Carlo simulation of the scattering and energy loss of relativistic electrons respectively positrons in matter [9]. Modified versions of RELECN and RELPOSN appear as subroutines in the programs (1)-(4). The multiple scattering and energy loss models used in RELECN and RELPOSN are briefly indicated in Appendix 1.

Experimental singles electron spectra

Fig.7 shows experimental singles spectra, i.e., the number of electrons at different energies recorded by the spectrometer on the same side of the thorium foil as the source (the backscattering spectrum B) and the number of electrons recorded by the spectrometer on the other side (the transmission spectrum T), with the same measuring time at all settings. The figure also indicates the sum $T + B$. This experimental sum spectrum may be compared to the theoretical beta-spectrum given by

$$\beta(E) = [\beta_1(E) + \beta_2(E)] \cdot w(E) \tag{2}$$

and shown in Fig.8. Here, $w(E)$ is a factor proportional to the energy window corresponding to the energy resolution of the spectrometer. This factor is determined by the fact that the relative momentum resolution is fixed to 4.5 % (cf. above). From

$$E_t^2 = p^2c^2 + (m_oc^2)^2 \tag{3}$$

where E_t is the total energy, p the momentum and m_o the rest mass, differentiation gives

$$dE = [E_t - (m_oc^2)^2/E_t] \cdot (dp/p) \tag{4}$$

from which

$$w(E) \propto (E_t - (m_oc^2)^2/E_t) \tag{5}$$

This way of including the spectrometer profile (by multiplication with a factor $w(E)$) is valid if the energy distribution varies negligibly over an energy interval corresponding to the resolution. It is seen that the spectrum in Fig.8 is somewhat different from the sum spectrum in Fig.7 in the energy range of interest; i.e. the energy distribution is influenced, presumably by scattering and energy loss. There is a drastic difference between the T and Fig.8 spectra on one hand, and the B spectrum on the other. The shape of the B spectrum can be qualitatively understood from the fact that electrons with higher energy have a longer transport mean free path; they will therefore with larger probability be transmitted through the foil, and thus be lost as contributors to the backscattering. Therefore, while energy loss in the foil may not be large, it will mainly be the low energy part of the β-spectrum that contributes to the backscattering from the foil.

Simulation of singles electron spectra - program S

Program S has the structure shown in Fig.9a. The flow diagram is shown in Fig.9b. Fig.10 indicates the scattering geometry. The subroutines B1START and B2START sample the energy and initial (random) direction of motion for an electron emitted in the β_1 or the β_2 decay, respectively. The subroutines ELSIM1, ELSIMH and ELSIM2 are all modified versions of RELECN. ELSIM1 simulates the scattering of an electron penetrating into the bottom of the cavity. ELSIMH simulates the scattering of an electron in the cylindrical walls of the source holder (assuming the cavity wall to be flat rather than cylindrical on the spatial scale of a typical electron trajectory in the wall). In both cases it is assumed that the scattering material is iron, which is close enough to steel for the present calculations. ELSIM2 simulates the scattering of an electron in the thorium foil. A particular electron might for example first hit the cavity wall and be scattered out again, and then hit and penetrate the thorium foil (Fig.10). In this case, the multiple scattering history is treated by ELSIMH and ELSIM2 in succession.

In order to avoid a computational complexity which would not be motivated in view of the lack of correspondingly precise knowledge of the electron-optical geometry, the following approximations are made:

1) The source is assumed to be situated at a point in the centre of the bottom of the cavity (Fig.10).

2) Electrons which are scattered against the cylindrical cavity walls and then hit the source holder (the cavity walls or bottom) a second time are discarded, i.e. their simulation histories are terminated. This approximation may be discussed by means of the following estimate.

Assume that, say, N electrons are emitted by the source, including in the following argument also those which have started inwards and are backscattered from the bottom of the cavity. Roughly $0.1 \cdot N$ electrons will hit the foil directly, while the remaining $0.9 \cdot N$ electrons hit the cavity walls. The backscattering from the cavity walls is expected to be roughly 30 %, and the probability that such a backscattered electron will hit the foil directly should be about 10 - 20 %, say 20 %. Thus the number of electrons that hit the foil directly, or after at most one scattering against the cavity walls, should be roughly

$$(0.1 + 0.9 \cdot 0.3 \cdot 0.2) \cdot N \approx (0.1 + 0.05) \cdot N$$

This indicates that the number of recorded electrons which hit the foil after being scattered against the cavity walls should be about half the number which hit directly. (Actually, the simulations below indicate that the value is smaller.) The number of electrons which hit the source holder (cavity walls or bottom) a second time should be about $(0.9 \cdot 0.3 \cdot (1 - 0.2)) \cdot N \approx 0.2 \cdot N$. If we again estimate that 30 % of these are backscattered out of the source holder, and that 20 % of these backscattered electrons hit the foil, we find that the number of electrons which hit the foil after two successive scatterings in the source holder should be roughly $0.2 \cdot 0.3 \cdot 0.2 \cdot N \approx 0.01 \cdot N$. If we disregard electrons which have hit the source holder three times or more, we thus find that out of all electrons reaching the foil, the fraction which have reached the foil after at most one scattering against the source holder should be about $0.15/(0.15 + 0.01) \approx 94$ %.

We may extend this estimate to the coincidence matrix resulting from the E0 decay as follows. We first apply the same argument to the positrons, to find approximately the same values. Then, neglecting the correlation between the directions of motion of the electron and the positron, simple probability sums and products give the following estimates of the relative contributions to the coincidence matrix. The notation (j,k) means here that the number of scatterings against the source holder is j for one lepton in a pair and k for the other (not counting the initial backscattering from the bottom of the cavity of those leptons which start inwards from the source):

(0,0) ... relative contribution $0.1 \cdot 0.1 = 0.01$
(0,1) ... relative contribution $2 \cdot (0.1 \cdot 0.05) = 0.01$
(1,1) ... relative contribution $0.05 \cdot 0.05 = 0.0025$
(0,2) ... relative contribution $2 \cdot (0.1 \cdot 0.01) = 0.002$
(1,2) ... relative contribution $2 \cdot (0.05 \cdot 0.01) = 0.001$
(2,2) ... relative contribution $0.01 \cdot 0.01 = 0.0001$

According to simulations to be described below, up to about 40 % of the E0 coincidence matrix may be due to events where at least one lepton was scattered against the cavity walls, discarding leptons which have suffered further scattering against the source holder. This value is somewhat lower than that obtained from the above rough estimate, which gives $0.0125/0.0225 \approx 55$ %. The difference may in part be due to the neglect of the directional correlation.

The contribution from coincidence pairs where one or both leptons have been scattered once from the cavity walls and backscattered again from the cavity walls or bottom, is, according to the above estimate, about $0.0031/0.0256 = 12$ %. Since the singles spectrum simulations indicate that the above estimate exaggerates the magnitude of the contribution from leptons scattered from the cavity wall, this value is however probably too large. In addition, it may be noted that this neglected contribution to the coincidence matrix is two-fold smeared out by bulk backscattering energy loss, and therefore expected to be essentially flat.

3) All electrons hitting the foil at a distance $r < r_{eff}$ from the centre point (see Fig.10) are assumed to enter into one of the spectrometers, provided that they are transmitted through or backscattered from the foil within an angular interval $\theta_{min} < \theta < \theta_{max}$ relative to the normal to the respective foil surface. Electrons hitting the extended plane of the foil outside the radius r_{eff} are discarded.

In other words, r_{eff} is the effective radius of the electron (positron) source, as viewed from both spectrometers, and we assume that the contribution to the spectrometer luminosity per unit source area is constant within this effective radius. The effective radius should at most be equal to or, more likely, smaller than the physical size of the foil.

In the simulations, the angles θ_{min} and θ_{max} were, to obtain reasonable computation times, chosen as 10^0 and 50^0, respectively. This angular interval is centered at the same angle as the physical one ($\approx 30^0 \pm 3^0$), and avoids glancing angles, for which one may expect significantly different energy distributions. As will be seen, the use of this artificially enlarged solid angle of acceptance does not lead to significant changes in the shapes and relative magnitudes of the transmitted and backscattered energy loss distributions. Note that in the analysis [4] we need to consider only the relative magnitudes of the different simulated coincidence matrices; therefore, the artificially enlarged solid angle will not introduce any systematic error.

The spectrometer profile is assumed to be gaussian with a relative momentum resolution $\Delta p/p = 0.045$. It is taken into account by means of the following method. Initially the transmission and backscattering spectra T and B are set $= 0$ at all settings. Assume that an electron of kinetic energy E is emitted from the foil, in an angular interval appropriate for one of the spectrometers. Let the setting of this spectrometer be such as to nominally accept electrons with kinetic energy S. Then, the probability that this electron is actually detected is assumed to be proportional to a gaussian factor

$$g(S,E) = \exp\left[-\left(\frac{1.665(E-S)}{\Delta E}\right)^2\right] \tag{6}$$

where ΔE is the full width at half maximum of the spectrometer profile, given by

$$\Delta E = [S_t - (m_o c^2)^2/S_t] \cdot (\Delta p/p) \tag{7}$$

and

$$S_t = S + m_o c^2 \tag{8}$$

is the total energy corresponding to the spectrometer setting. If the electron is, say, transmitted, the program adds to the spectrum value $T(S)$ at each selected setting S a contribution $g(S,E)$ from this electron. The same procedure applies to a backscattered electron and the backscattering spectrum $B(S)$.

Several simulations were made with varying geometrical conditions. Results are exemplified in Figs.11a - d. The acceptance angle is here always $10^0 < \theta < 50^0$, except for one of the cases shown in Fig.11d.

The result with $r_{eff} = 2$ *mm* is shown in Fig.11a. The simulated transmission (T) energy distribution has been multiplied by a trivial scaling factor, so as to reproduce the average value of the experimental T distribution between the kinetic energies 200 keV and 850 keV. When the same scaling factor is applied to the backscattering (B) distribution, it is however found that multiplication with a further scaling factor $f \approx 0.73$ is required to get good agreement with the B distribution as well. We shall return to the discussion of the origin of the correction f below. It is seen that the agreement in shape between the experimental and simulated distributions is good. It should be remembered that the backscattered energy distribution has virtually no direct resemblance to the theoretical beta spectrum of Fig.8; i.e. the effect of the multiple scattering and energy loss is large and therefore the result should be sensitive to the simulation procedure.

Also included in Fig.11a is the contribution from electrons which have been scattered against the cavity walls. It is here very small, and it may be noted that the shape of the β spectrum is almost entirely smeared out. According to the simulations, 4.7 % of the electrons emitted from the source, or, after backscattering, from the bottom of the cavity, with energies between 200 keV and 850 keV, hit the foil directly within the effective radius (2 mm), while = 0.5 % hit after being scattered once against the cavity walls. The value 4.7 % is actually larger than the solid angle of the effective foil area as seen from the source, due to the nonisotropic angular distribution of the backscattered electrons (see below).

The result with $r_{eff} = 4$ mm is shown in Fig.11b. It may be noted that the factor f is somewhat smaller than in Fig.11a ($f = 0.7$, i.e. the required correction is somewhat larger) and that the contribution from

electrons which have been scattered against the cavity walls is also somewhat larger. The above-mentioned fractions are in this case 16.7 % and 1.8 %, respectively.

In Fig.11c the result with $r_{eff} = 10$ *mm* is shown. In this case, $f = 0.62$. The agreement with the transmission energy distributions appears to be somewhat better than in Fig.11b. The fraction of electrons with energies between 200 and 850 keV which hit the foil within r_{eff} directly is here 16.7 %, while the fraction which hit after being scattered once in the source holder is 4.9 %. The larger contribution from the indirect hits is apparent in the figure.

In fact, since the radius of the part of the foil which is seen directly from the source (cf. Fig.1) is very nearly 4 mm, it is clear that an increase of r_{eff} beyond this value will only increase the indirect (cavity-scattered) contribution in the simulations. The fraction of direct hits for different r_{eff} indicate an angular distribution of the form $\approx (\cos\theta)^{0.64}$, which is reasonable in view of that it should be a mixture of the isotropic angular distribution for those electrons which are emitted from the source in the outward direction (without scattering) and the (approximately) cosine distribution of those which are emitted in the inward direction and subsequently backscattered.

The total transmission and backscattering probabilities in the thorium foil in the energy range 200 - 850 keV, and into the angular interval $10^0 < \theta < 50^0$, were found to be about 29 % and 10 %, respectively.

Fig.11d shows a comparison, for the case of $r_{eff} = 5$ mm, between results obtained with the standard angular interval $10^0 - 50^0$ and a more narrow interval $25^0 - 35^0$. It is seen that the difference, using the same correction factor $f = 0.68$, *is* insignificant.

We now consider the origin of the correction factor f. Since a single (i.e. energy-independent) scaling factor is sufficient, it is likely to be due to the geometry of the experimental set-up, or to a feature of the apparatus which varies only negligibly with energy in the interval 200 - 850 keV. An - at least - partial geometrical explanation is readily found. The source holder (see Fig.1) is a cylinder of outer diameter 5 mm, pointing perpendicularly to the centre of the thorium foil on the backscattering (B) side. If the foil is viewed at an angle of 30^0 (approximately the acceptance angle) from this side, part of it is hidden by the source holder. The fraction of the foil which is hidden can be estimated from the geometry to be about 20 - 25 % (cf. Fig.1), which is somewhat less than required to explain the whole correction, the difference depending on the choice of r_{eff} in the simulation.

We thus find that f should be due to a difference in the luminosity of the two spectrometers, rather than to any error in the simulation, and that this difference is, at least to a large part, due to the shadowing effect of the source holder. The magnitude of this effect depends on the exact position of the foil, and the final correction f also depends on any further details which influence the ratio of the luminosities of the two spectrometers, for example the orientation of the two electron-optical baffle systems with respect to the (rectangular) foil and the performance of the two electron detectors.

The correction f does not enter into the analysis in Ref.[4], where different coincidence matrices are compared with each other, for the reason that f, if explicitly included, will in effect act as a reduction of the luminosity of one spectrometer, and will therefore be present as a common multiplicative factor in all the simulated matrices.

We therefore conclude that the agreement obtained between the shape of the measured and the simulated singles spectra in transmission and backscattering indicates that the simulation of multiple scattering and energy loss, and the approximations made here as regards scattering geometry, are sufficiently accurate for the simulation of the coincidence matrices.

The value $r_{eff} = 10$ *mm*, as well as the sampling procedures of Program S described above, were adopted in the subsequent simulations of the coincidence matrices. This rather large r_{eff} value was chosen for the reason that it is expected to give a better statistical efficiency than, say, $r_{eff} = 2$ *mm*, while it gives equally good agreement with the experimental energy distributions.

Simulation of electron-positron coincidences from the E0 decay - Program E

The structure of program E is seen in Fig.12a, and the flow diagram in Fig.12b. The subroutine E0START simulates the initial energies and directions of motion of the electron and the positron, using the distribution $P_{E0}(E_{t1}, G)$. For each electron-positron pair thus starting in the source, the multiple scattering history of the electron is simulated first; the positron scattering history is initiated only if the electron is backscattered from the foil with sufficient energy (i.e. sufficient to give a non-negligible contribution to the coincidence matrix, considering the spectrometer response) and inside the acceptable angular interval. As in Program S, the subroutines ELSIM1 (POSIM1), ELSIMH (POSIMH) and ELSIM2 (POSIM2) handle the simulation of multiple scattering and energy loss of the electron (positron) in, respectively, the source backing, the cylindrical cavity walls of the source holder, and the thorium foil. A coincidence is recorded by program E if the electron is backscattered from the thorium foil with a kinetic energy above a cut-off value = 0.15 MeV within an angular interval $10^0 - 50^0$ relative to the backscattering surface normal, while, for the same pair, the positron is transmitted through the foil, likewise with kinetic energy > 0.15 MeV and within the angular interval $10^0 - 50^0$ relative to the transmission surface normal.

The output file is a list of the final kinetic electron and positron energies E_e and E_p (as well as further data) for all the recorded coincident pairs. This file is read by a second program COINE0S, which
1) initiates the coincidence matrix, setting all matrix elements $M_{E0}(S_e, S_p) = 0$;
2) discards all coincidences where any lepton has hit the thorium foil outside the effective radius r_{eff} (= 10 mm)
3) for each accepted pair, and at all combinations of settings S_e and S_p, adds the quantity $g(S_e, E_e) \cdot g(S_p, E_p)$ to the matrix element $M_{E0}(S_e, S_p)$. (See Eq.(6).)

Thus, the electron-positron coincidence matrix is obtained by adding together the contributions from all pairs to all matrix elements.

It should be mentioned that all the simulated coincidence matrices presented here are "renormalized" by dividing each element with a factor C. This factor C is the same for all the matrices, and is taken to be the approximate average value of the sum of all matrix elements for a matrix containing a *single* coincident pair. The purpose of the "renormalization" is merely to give the matrix elements a convenient magnitude corresponding to the number of coincident pairs contributing to the matrix.

The number of starting pairs (i.e., simulated E0 decays resulting in electron-positron pairs) was $8 \cdot 10^7$. With r_{eff} = 10 mm, this resulted in $6.5 \cdot 10^4$ coincidences.

The relative number of accepted coincidences where the electron as well as the positron did hit the thorium foil with energy above cut-off and without prior scattering against the source holder was, as discussed previously, found to be about 40 %.

The E0 coincidence matrix obtained with r_{eff} = 10 mm for $8 \cdot 10^7$ starting pairs is shown in Fig.13. Fig.14 shows the E0 matrix schematically (by contour lines) for a case of $2 \cdot 10^7$ starting pairs. Fig.14a shows the full E0 matrix. Fig.14b shows the E0 coincidence matrix obtained if only those coincidences are retained where the electron or the positron or both have been scattered against the source holder; the smearing effect on the energy loss distribution is evident. Fig.14c shows the difference between Fig.14a and Fig.14b, i.e. the coincidence matrix obtained if only pairs, where both particles have hit the thorium foil directly, are recorded. The ridge corresponding to the fixed sum energy of the electron and positron in the E0 decay is, as expected, sharper in Fig.14c than in Fig.14a.

Figs.13 and 14 show that there is a tendency for the positron in a coincident pair to have a higher energy than the electron. This asymmetry apparently depends on the fact that we record *backscattered* electrons but *transmitted* positrons. For example, an electron hitting the foil with a higher energy will have a larger probability of being transmitted, and a smaller probability of being backscattered, while a positron hitting the foil with lower energy will have a smaller probability to be transmitted.

Simulation of the Møller scattering coincidence matrix - program M.

The structure of program M is shown in Fig.15. The subroutines B1START and B2START simulate the initial energy and initial direction of motion of an electron from the β_1 or β_2 decay, and the subroutines ELSIM1 and ELSIMH simulate the possible scattering of this electron in the backing behind the source and in the source holder (i.e. the same procedures as in Program S).

The subroutine ELSIM2 simulates the scattering of the electron in the thorium foil (in the case that the foil is hit), with the following special feature: the cross section for Møller scattering with an energy transfer above a certain limit is artificially increased by a factor 200. When such a Møller collision occurs, the energies and directions of motion of both electrons after the collision, as well as the location of the event, are stored in memory. (The directions of motion are calculated by the subroutine DIRCOL on basis of the conservation of total energy and momentum.) However, the Møller event is treated as real, in the sense that it causes a change in the energy and direction of motion of the "primary" electron, only with the probability 1/200. In any case (whether the Møller event is treated as real or not), the "primary" electron continues its trajectory through the foil, until being absorbed (i.e., reaching a cut-off energy) or emitted from the foil. In the latter case, the emitted electron is *not* recorded; its only purpose has been to produce statistically well-distributed Møller events in the foil. The value 200 is chosen so as to result in an average of approximately one Møller event per primary trajectory; it should be observed that more than one event in a trajectory may be produced, and that allowance for this possibility is necessary to avoid a distorted distribution . (The same procedure was used to simulate Bhabha scattering in Ref.[3].)

When one "primary" electron scattering history has been terminated, the subroutine ELSIM3 simulates the subsequent scattering of each of the two electrons starting from each artifical Møller event generated during that scattering history (provided that both electrons initially have sufficient energies). If, then, the electrons from a particular event escape from opposite sides of the foil, with sufficient energies and into the selected acceptance angle ($10^0 - 50^0$), an electron-electron coincidence is recorded.

The resulting list of coincident electron pairs is treated by the program COINMOS, which (in the same way as COINE0S) introduces the effect of the gaussian spectrometer profiles and constructs the coincidence matrix (including the renormalizing factor C). The resulting matrix $M_M(S_B, S_T)$ (where B and T indicate backscattered and transmitted electrons, respectively) is shown in Fig.16a. In Fig.16b, it has been scaled so as to be $= 1$ in the centre and schematically compared with likewise scaled experimental data in Fig.16b.

Simulation of matrices due to hypothetical events - program H

The hypothetical event here is [2 - 4] that a positron and an electron start simultaneously in opposite but otherwise random directions from a randomly selected position in the thorium foil, both with energies in the vicinity of 330 keV. The subsequent simulation of the scattering histories is quite straight-forward. Both leptons are scattered in the thorium foil. Provided that the positron escapes with sufficient energy and within the (artificially enlarged) acceptance angle on the side of the positron spectrometer, while simultaneously the electron likewise escapes on the side of the electron spectrometer, a coincidence is recorded. The list of coincidences is treated by a program, which in the same way as COINE0S and COINMOS applies the spectrometer profiles and constructs the coincidence matrix $M_H(S_e, S_p)$. For the analysis [4], 29 such coincidence matrices were produced, differing only in a variation of the initial energy of the two leptons along the diagonal of the coincidence matrix. One such matrix is shown in Fig.17.

Synthesis of simulated results

The result of the simulations is essentially the following simulated coincidence matrices:

1) The E0-decay coincidence matrix $M_{E0}(S_e, S_p)$
2) The Møller coincidence matrix $M_M(S_B, S_T)$
3) The hypothetical event coincidence matrix $M_H(S_e, S_p)$ (i.e., 29 matrices)

In the comparison with experimental data, we have to consider the proper normalization of these matrices relative to each other. They have been generated with identical geometrical conditions, i.e. as regards acceptance angles, spectrometer profiles, foil thickness and source geometry. Thus, we have to renormalize with respect to the appropriate number of starting electrons or electron-positron pairs in each case.

In program H, the number of starting electron-positron pairs was 10^4 for each of the 29 matrices.

In program M, the number of starting beta particles was 10^7, corresponding to $5 \cdot 10^6$ ^{90}Sr decays (see Fig.2; we neglect β_3). However, taking account of the artificial enhancement of the Møller cross section (by the factor 200), the appropriate number of decays is $200 \cdot 5 \cdot 10^6$.

In program E, the number of starting electron-positron pairs was $8 \cdot 10^6$. In the decay scheme (Fig.2) there is for each ^{90}Sr decay the following number of electron-positron pairs from the E0-decay:

$$\frac{0.011}{100} \cdot 0.31 = 3.41 \cdot 10^{-5}$$

(i.e. the product of the branching ratio and the relative number of pairs created in the E0 decay). Thus the number of ^{90}Sr decays corresponding to the simulation is $80 \cdot 10^6/3.41 \cdot 10^{-5}$.

It follows that when comparing the E0 matrix and the Møller matrix, one should, to obtain the proper relative magnitudes on basis of the same number of ^{90}Sr decays, multiply the E0 matrix by

$$\frac{200 \cdot 5 \cdot 10^6}{80 \cdot 10^6/3.41 \cdot 10^{-5}} = 0.426 \cdot 10^{-3}$$

For further discussion of the use of the simulated data in the analysis, we refer back to Ref.[4].

Appendix

The FORTRAN codes RELECN and RELPOSN, which were used for simulating the penetration of electrons and positrons through matter in the present work, have been described in Ref.[9]. A correction as regards elastic scattering has later been introduced, using data from Ref.[10].

The principle of the RELECN flow diagram is shown in Fig.18; the RELPOSN diagram is similar, differing only in certain details [9].

The elastic scattering process is simulated using a substitute scattering process with the same transport mean free path λ_{tr}, but with an elastic mean free path λ_e which is one or a few orders of magnitude larger than that of the real process. Conditions for the validity of this method are discussed elsewhere (see [9,10] and references therein). The substitute process has a fixed elastic mean free path (taken to be at least an order of magnitude smaller than the typical thicknesses to be traversed) and a single scattering angular distribution which has the form of the screened Rutherford differential cross section with an adjusted, energy-dependent screening parameter [9,10].

The value of λ_{tr} is computed on basis of the differential cross section obtained by relativistic (Dirac) partial wave analysis of the elastic scattering of electrons and positrons in the nuclear Coulomb potential screened by atomic electrons [10].

Energy loss due to electronic as well as radiative collisions are simulated using the partial CSDA approach (CSDA = Continuous Slowing Down Approximation). This approach consists in treating collisions with energy transfer W above a certain limit W_{min} as discrete events, while collisions with energy transfer below this limit are treated as a continuous average energy loss along the trajectory.

The total average electronic energy loss per unit path length (electronic stopping power) is assumed to be given by the relativistic Bethe-Bloch formula, using the mean ionization potential I as a material constant. Electronic collisions with energy transfers $W > W_{min}$ are simulated as discrete events on basis of the Møller cross section. The stopping power corresponding to the Møller cross section (= mean energy transfer divided by mean free path) is subtracted from the total electronic stopping power, giving the contribution from electronic collisions to the partial CSDA stopping power.

A similar procedure is used for radiative losses. For positrons, the total stopping power formula is slightly modified, and - related to this - the Møller cross section is replaced by the Bhabha cross section.

The step length between discrete events is random-sampled (see e.g. ref.[9]) in accordance with the mean free path λ, which is given by

$$\frac{1}{\lambda} = \frac{1}{\lambda_e} + \frac{1}{\lambda_i}$$

where λ_e, as mentioned, is the mean free path between the elastic events of the (substitute) elastic process, and λ_i is the mean free path between discrete inelastic events. The partial CSDA stopping power is multiplied by the simulated step length to the next discrete event (elastic or inelastic) to give the partial CSDA energy loss during a step. The discrete event is elastic with a probability λ/λ_e, otherwise inelastic. (See Fig.18.)

The source holder was assumed to consist of iron, as regards scattering and energy loss, with a mean ionization potential $I = 280$ eV. The thorium of the foil was assumed to have the mean ionization potential $I = 870$ eV.

References

[1] K.A.Erb, I.Y.Lee and W.T.Milner, Phys.Lett.B **181**, 52 (1986).

[2] Chr.Bargholtz, L.Holmberg, K.E.Johansson, D.Liljequist, P.-E.Tegnér, L.Bergström and H.Rubinstein, J.Phys.G **13**, L265 (1987).

[3] Chr.Bargholtz, L.Holmberg, K.E.Johansson, D.Liljequist, P.-E.Tegnér and D.Vojdani, Phys.Rev.C **40**, 1188 (1989).

[4] Chr.Bargholtz, L.Holmberg, D.Liljequist, P.-E.Tegnér and D.Vojdani, Phys.Rev.C **48**, 1388 (1993)

[5] B.S.Dzjelepov, L.N.Zyrjanova and J.P.Suslov, Betaprotsessy, Akad. Nauk SSSR, Leningrad 1972

[6] S.DeBenedetti, Nuclear Interactions, Wiley, New York, 1964, p.415

[7] Ch.Hoffman, J.Reinhardt, W.Greiner, P.Schlüter and G.Soff, Phys.Rev.C **42**, 2632 (1990)

[8] D.Liljequist, J.Phys.D.: Appl.Phys. **10**, 1363 (1977).

[9] M.Ismail and D.Liljequist, University of Stockholm Institute of Physics report USIP 86-11.

[10] D.Liljequist, M.Ismail, F.Salvat, R.Mayol and J.D.Martinez, J.Appl.Phys.**68**, 3061 (1990)

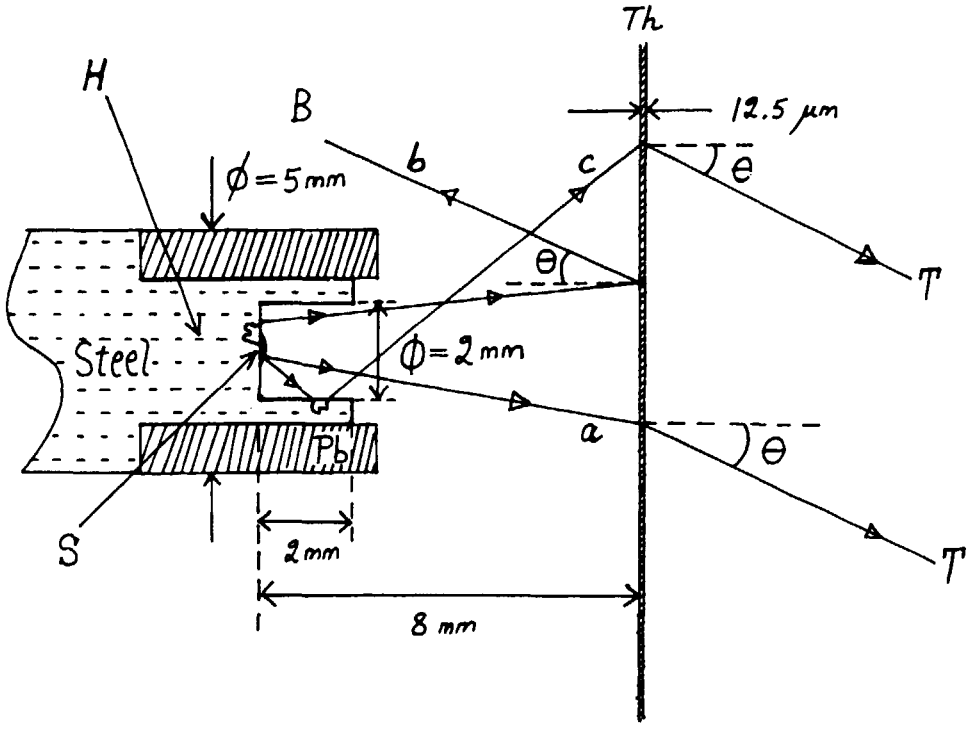

Fig.1 Experimental geometry. S = source, H = source holder (cylindrical), Th = thorium foil, B = backscattered lepton, T = transmitted lepton, θ = acceptance angle. A few electron (or positron) trajectories are schematically indicated. Trajectory (a): direct hit of foil and transmission; trajectory (b): backscattering from bottom of cavity, foil hit, and backscattering; trajectory (c): scattering from cavity wall, foil hit, and transmission.

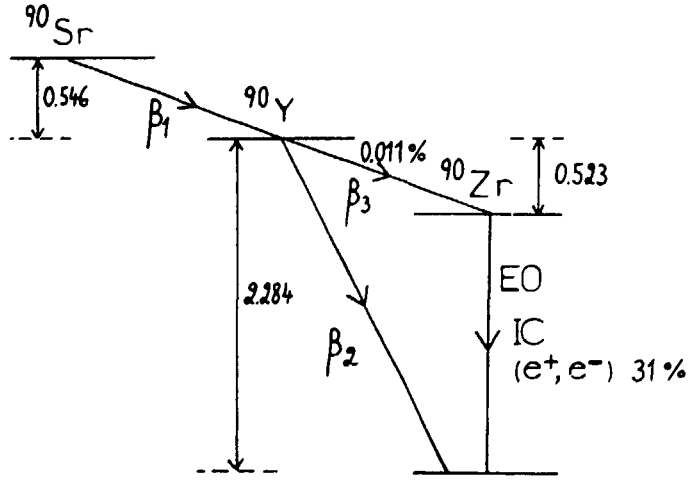

Fig.2 Decay scheme. Energies are in MeV.

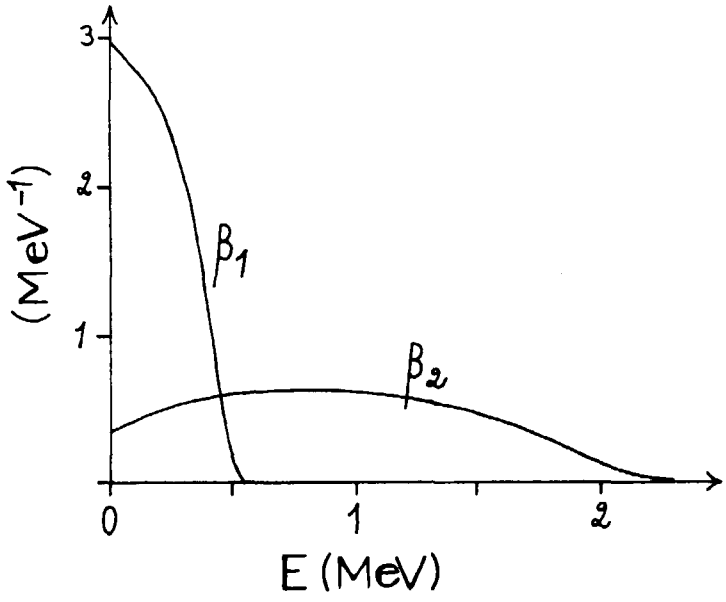

Fig.3 The β_1 and β_2 energy distributions (number of electrons per unit energy), each normalized to unit area.

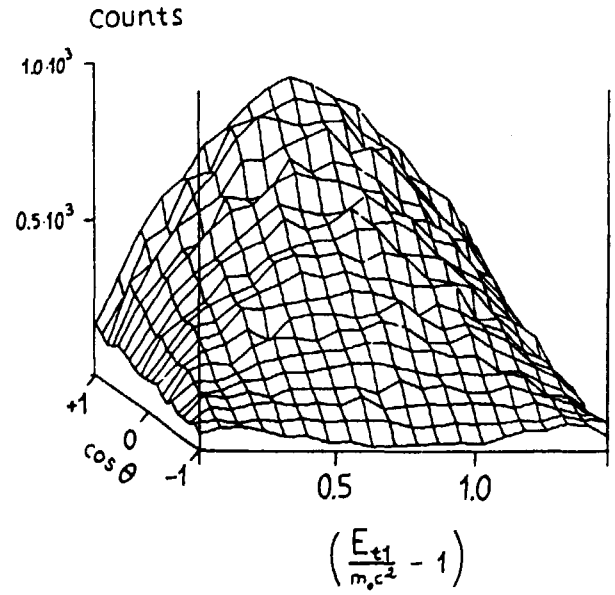

Fig.4 Sampling test (using the rejection method) of the energy-direction distribution $P_{E0}(E_{t1}, \cos\theta)$ of the electron and positron pair created in the E0 decay. E_{t1} is the energy of one lepton, θ is the angle between the directions of motions.

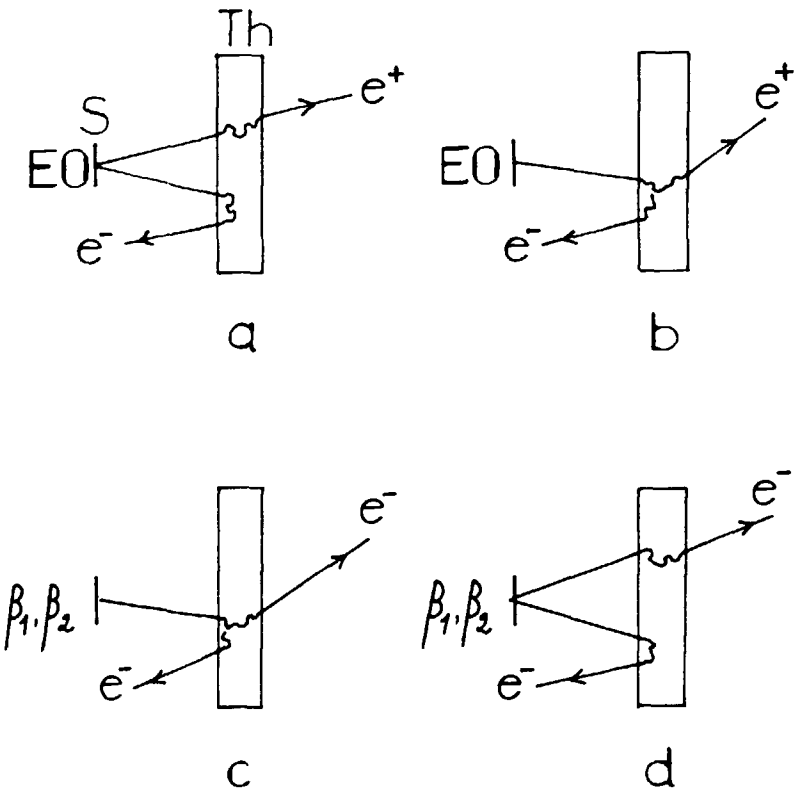

Fig.5 Schematic illustration of different scattering processes in the thorium foil.
a) Scattering from E0 decay, giving positron-electron coincidence.
b) Positron-electron coincidence due to Bhabha scattering.
c) Electron-electron coincidence due to Møller scattering. The β_1 and β_2 decays provide essentially all electrons for this.
d) Scattering influencing the transmission and backscattering singles spectra of electrons.

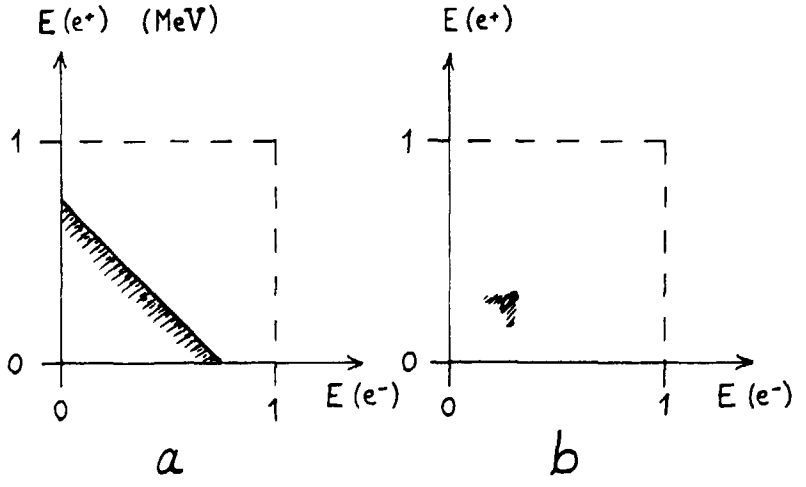

Fig.6 a) Schematic expected structure of positron-electron coincidence matrix due to E0 decay. Shading indicates effect of energy loss. b) Schematic expected structure of positron-electron coincidence matrix due to hypothetical events.

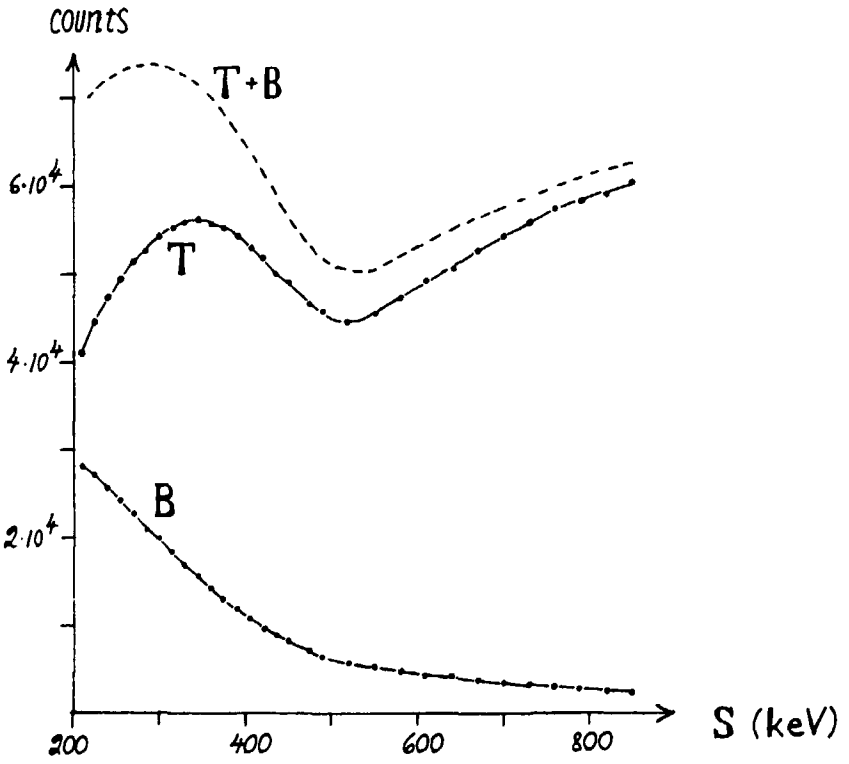

Fig.7 Experimental singles electron spectra $T(S)$ (transmission through the thorium foil) and $B(S)$ (back-scattering from the foil), i.e. number of recorded electrons at different spectrometer settings S. Results are shown as dots, joined, for convenience, by curves. The experimental sum spectrum $T + B$ is also indicated (dashed).

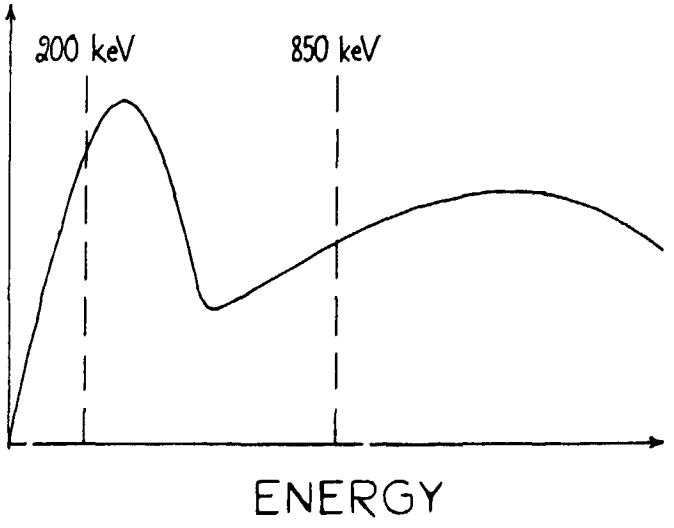

Fig.8 Sum of the theoretical β spectra from Fig.3 with correction $w(E)$ for the spectrometer resolution.

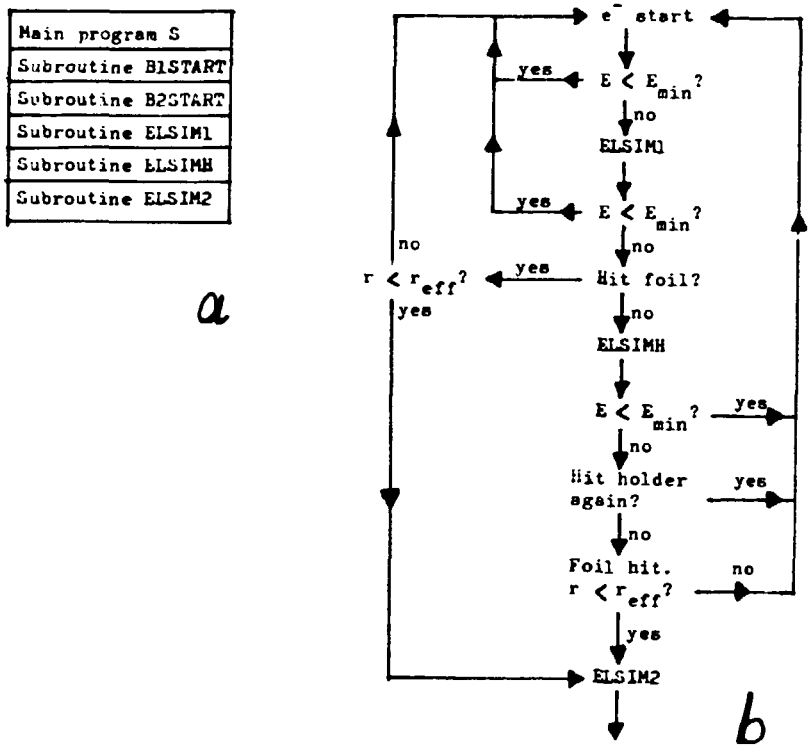

Fig.9 a) Structure of Program S. b) Flow diagram of Program S.

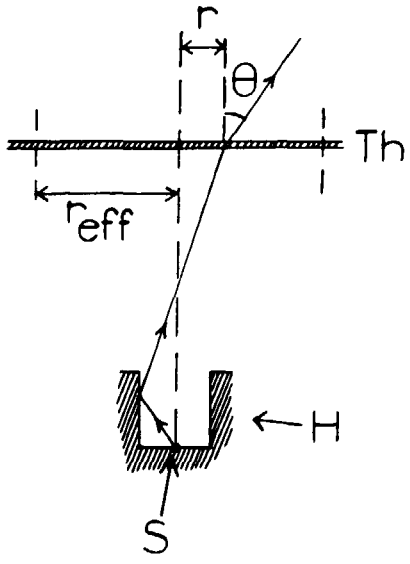

Fig.10 Scattering geometry of source holder and foil. An example of a possible scattering sequence is shown. The distance r from the foil hit point to the foil center is indicated. Notations otherwise as in Fig.1.

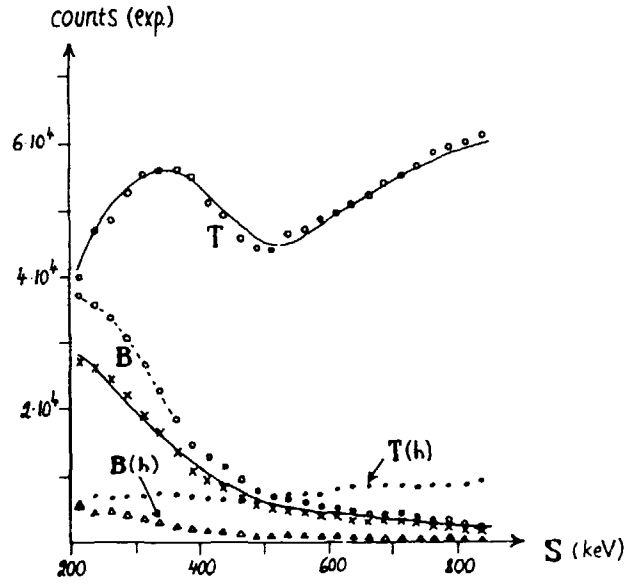

Fig.11a. Transmission (T) and backscattering (B) singles spectra. Experimental data (from Fig.7) are shown as full curves. Simulated spectra (shown as circles) have been obtained assuming the effective foil radius $r_{eff} = 2$ mm, with scaling to the experimental T curve. The number of starting simulated electrons (β_1 or β_2 decay, see Fig.2) was $4 \cdot 10^6$. The simulated number of electrons escaping from the transmission side of the thorium foil with energies between 200 and 850 keV, and at angles between 10^0 and 50^0 relative to the foil normal, was 18924. Crosses show the simulated B spectrum multiplied by the correction factor $f = 0.73$. Also shown are the simulated contributions T(h) and B(h) to T and B, respectively, from electrons scattered against the walls of the source holder cavity.

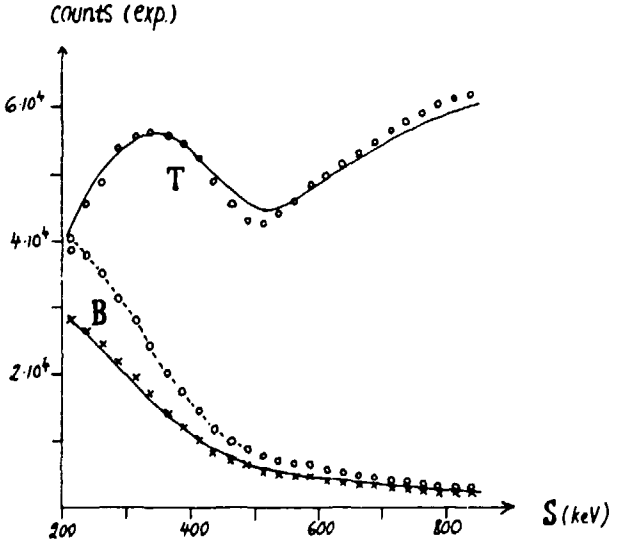

Fig.11b. Simulated singles spectra compared with experimental, for the case $r_{eff} = 4$ mm. Symbols are as in Fig.11a, and $f = 0.70$. The number of starting simulated electrons was 10^7.

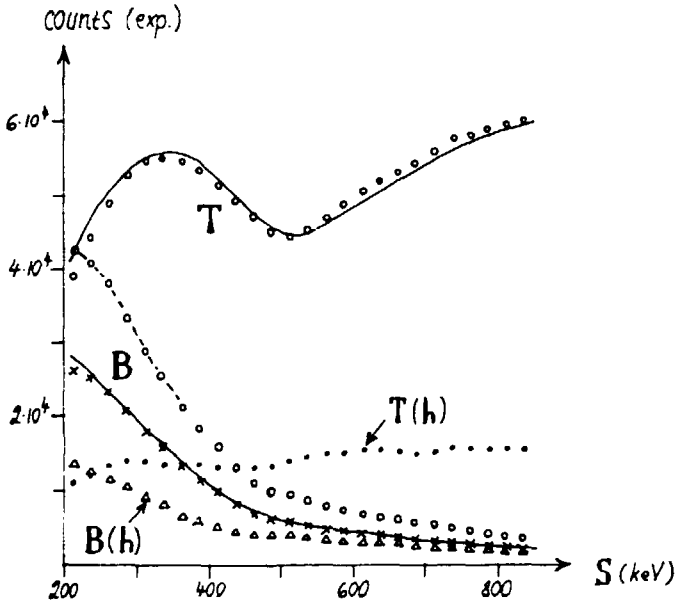

Fig.11c. Simulated singles spectra compared with experimental, for the case $r_{eff} = 10$ mm. Symbols are as in Fig.11a, and $f = 0.62$. The number of starting simulated electrons was $5 \cdot 10^6$.

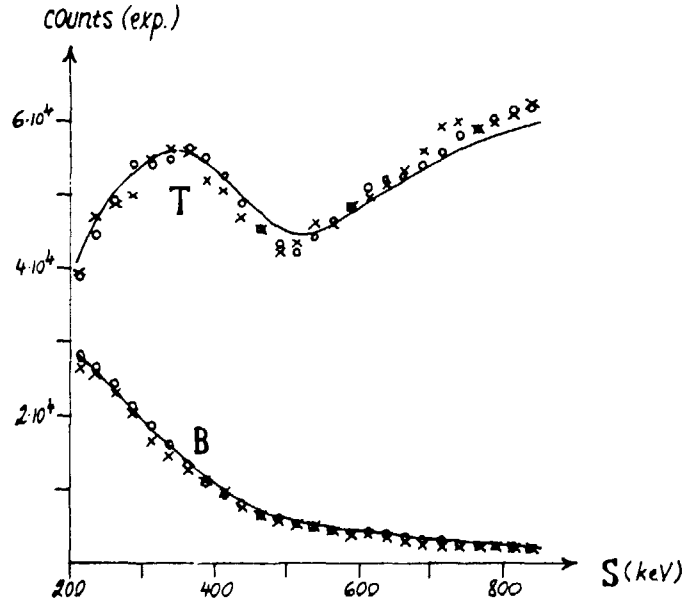

Fig.11d Simulated singles spectra compared with experimental, for the case $r_{eff} = 5$ mm. Circles show simulated results for the angular interval of acceptance $10^0 < \theta < 50^0$, while crosses show simulated results for $25^0 < \theta < 35^0$. In both cases, $f = 0.68$. Full curves are experimental data from Fig.7. The number of starting simulated electrons was $4 \cdot 10^6$ in each case.

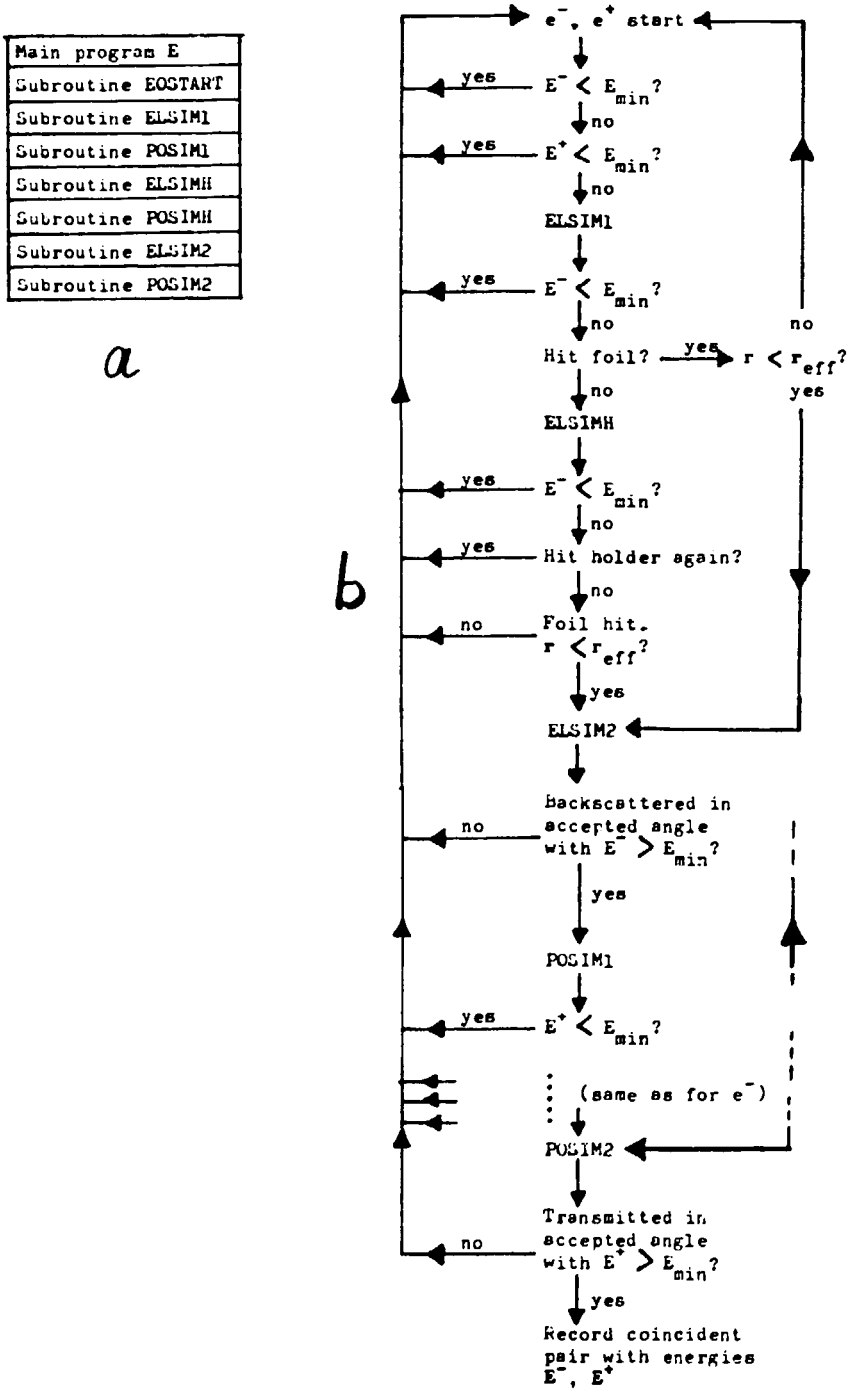

Fig.12 a) Structure of program E. b) Flow diagram of program E.

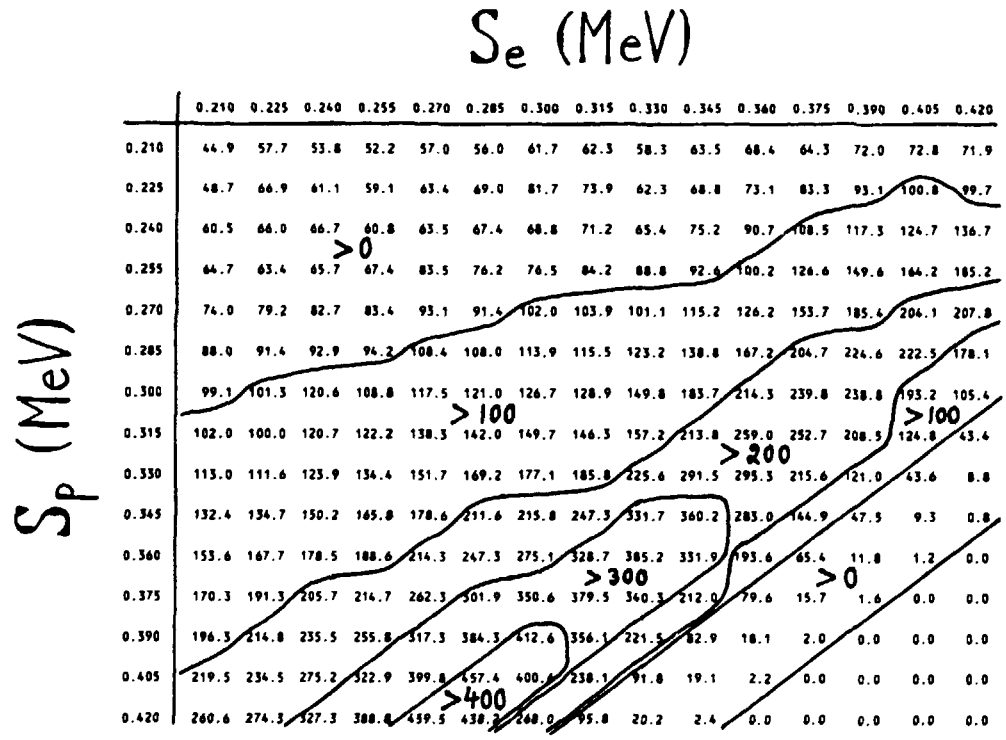

Fig.13 Simulated E0 matrix $M_{E0}(S_e, S_p)$ for $8 \cdot 10^7$ starting electron-positron pairs.

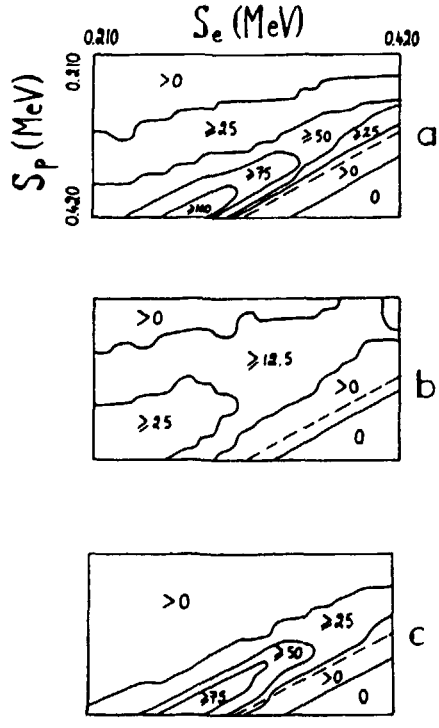

Fig.14 Simulated E0 matrices for $2 \cdot 10^7$ starting pairs, indicated by contour lines.
a) The complete E0 matrix.
b) E0 matrix obtained from those events where the electron or the positron or both have been scattered against the source holder.
c) Difference matrix, i.e. [(a) - (b)]. The dashed lines indicate the sum energy, i.e. the matrix in abscence of energy loss.

Main program M
Subroutine BISTART
Subroutine B2START
Subroutine ELSIM1
Subroutine ELSIMH
Subroutine ELSIM2
Subroutine ELSIM3
Subroutine DIRCOL

Fig.15 Structure of program M.

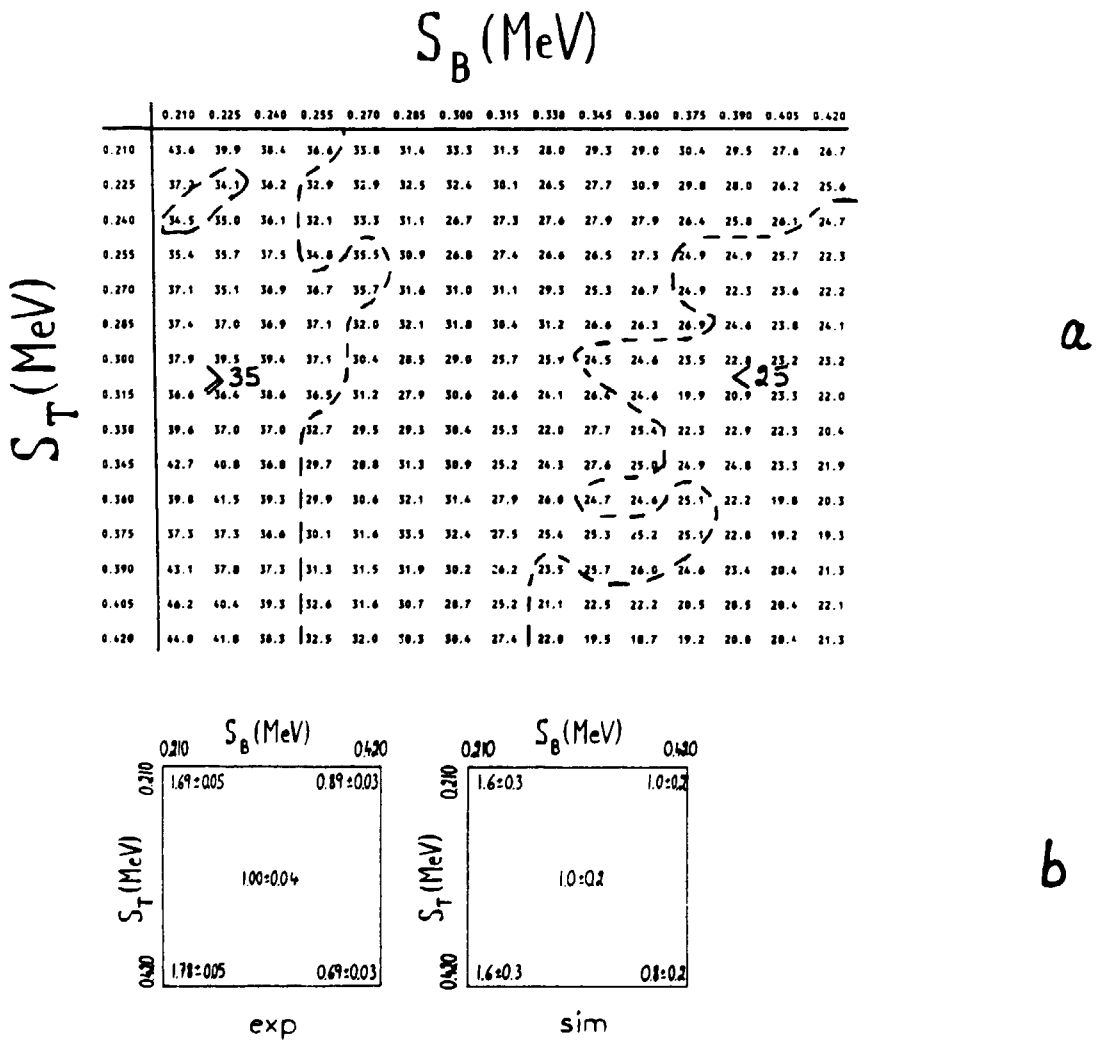

Fig.16 a) Simulated Møller coincidence matrix $M_M(S_B, S_T)$. b) Rescaled simulated and experimental Møller coincidence matrices. Values in the center and the corners are indicated with estimated statistical errors.

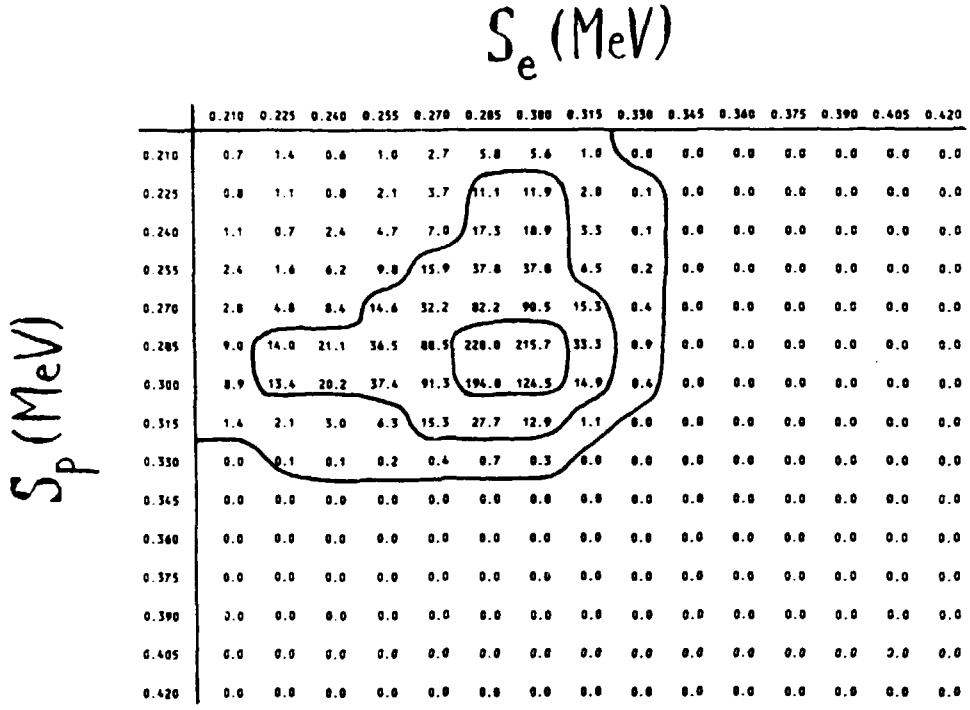

Fig.17 Example of a simulated electron-positron coincidence matrix $M_H(S_e, S_p)$ due to hypothetical events. In the case shown, the initial energies of the electron and the positron are both 300 keV.

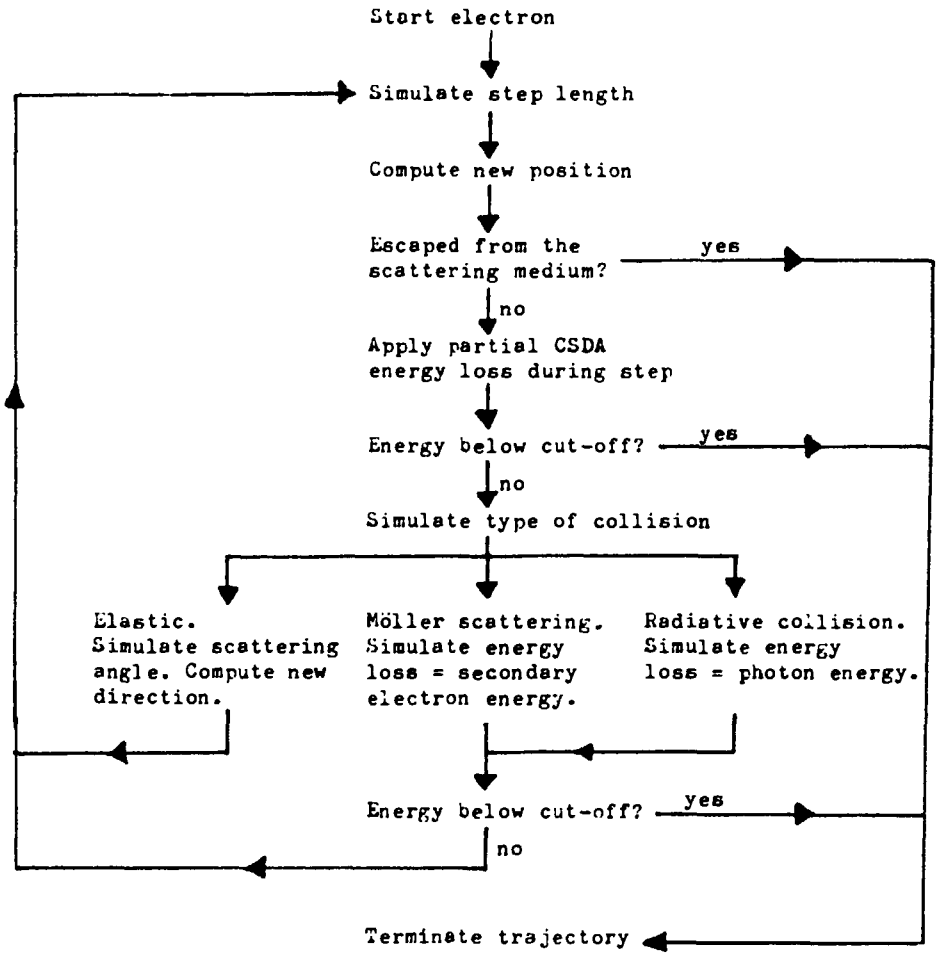

Fig.18 Principal flow diagram of RELECN, i.e. the basic principle of a typical scattering and energy loss subroutine (e.g. ELSIM1).